



Article scientifique

Article

2016

Accepted version

Open Access

This is an author manuscript post-peer-reviewing (accepted version) of the original publication. The layout of the published version may differ .

---

## Enolate Stabilization by Anion- $\pi$ Interactions: Deuterium Exchange in Malonate Dilactones on $\pi$ -Acidic Surfaces

---

Miros, François; Zhao, Yingjie; Sargsyan, Gevorg; Pupier, Marion; Besnard, Céline; Beuchat, Cesar; Mareda, Jiri; Sakai, Naomi; Matile, Stefan

### How to cite

MIROS, François et al. Enolate Stabilization by Anion- $\pi$  Interactions: Deuterium Exchange in Malonate Dilactones on  $\pi$ -Acidic Surfaces. In: Chemistry, 2016, vol. 22, n° 8, p. 2648–2657. doi: 10.1002/chem.201504008

This publication URL: <https://archive-ouverte.unige.ch/unige:80715>

Publication DOI: [10.1002/chem.201504008](https://doi.org/10.1002/chem.201504008)

## Supramolecular Chemistry

Enolate Stabilization by Anion- $\pi$  Interactions: Deuterium Exchange in Malonate Dilactones on  $\pi$ -Acidic Surfaces

François N. Miros, Yingjie Zhao, Gevorg Sargsyan, Marion Pupier, Céline Besnard, César Beuchat, Jiri Mareda, Naomi Sakai and Stefan Matile\*

**Abstract:** Enolate chemistry is an attractive topic to elaborate on possible contributions of anion- $\pi$  interactions to catalysis because of its central importance in chemistry and biology. To demonstrate the existence of such contributions, experimental evidence for the stabilization of not only anions but also anionic intermediates and transition states on  $\pi$ -acidic aromatic surfaces is decisive. To tackle this challenge for enolate chemistry with maximal precision and minimal ambiguity, malonate dilactones are covalently positioned on the  $\pi$ -acidic surface of naphthalenediimides (NDIs). Their presence is directly visible in upfield shifts of the  $\alpha$  protons in the  $^1\text{H}$  NMR spectra. The reactivity of these protons on  $\pi$ -acidic surfaces is measured by hydrogen-deuterium (H-D) exchange for 11 different examples, excluding controls. The velocity of H-D exchange increases with  $\pi$ -acidity (NDI core substituents:  $\text{SO}_2\text{R} > \text{SOR} > \text{H} > \text{OR} > \text{OR}/\text{NR}_2 > \text{SR} > \text{NR}_2$ ). H-D exchange kinetics vary with the structure of the enolate

(malonates > methylmalonates, dilactones > dithiolactones). Moreover, they depend on the distance to the  $\pi$  surface (bridge length: 11  $\gg$  13 atoms). Most importantly, H-D exchange depends strongly on the chirality of the  $\pi$  surface (chiral sulfoxides as core substituents; the crystal structure of the enantiopure (*R,R,P*)-macrocycle is reported). For maximal  $\pi$  acidity, transition-state stabilizations up to -18.8 kJ/mol are obtained for H-D exchange. The Brønsted acidity of the enols increases strongly with  $\pi$  acidity of the aromatic surface, the lowest measured  $\text{p}K_{\text{a}} = 10.9$  calculates to a  $\Delta\text{p}K_{\text{a}} = -5.5$ . Corresponding to the deprotonation of arginine residues in neutral water, considered as “impossible” in biology, the found enolate- $\pi$  interactions are very important. The strong dependence of enolate stabilization on the unprecedented seven-component  $\pi$ -acidity gradient over almost 1 eV demonstrates quantitatively that such important anion- $\pi$  activities can be expected only from strong enough  $\pi$  acids.

## Introduction

Aromatic surfaces can interact with anions,<sup>[1-8]</sup> cations,<sup>[9,10]</sup> or both.<sup>[11,12]</sup> Cation- $\pi$  interactions are ubiquitous in chemistry and biology and participate in many important processes, including

catalysis.<sup>[9]</sup> Anion- $\pi$  interactions occur on  $\pi$ -acidic rather than  $\pi$ -basic aromatic surfaces.<sup>[1-8]</sup> Ionpair- $\pi$  interactions, i.e., cation- $\pi$  and anion- $\pi$  interactions on the same surface, have been proposed last year to occur best on polarized push-pull surfaces.<sup>[11,12]</sup>

Compared to cation- $\pi$  interactions, anion- $\pi$  interactions are much younger, less common in biology, less explored in chemistry, and their origins are more complex and remain subject of debate among theoreticians.<sup>[2-8]</sup> Here, the term anion- $\pi$  interaction is used exclusively to define the site of interaction, that is the  $\pi$  surface, with anion-plane distances around or preferably shorter than the sum of the respective Van-der-Waals radii, but without any implications on the nature of the interaction.<sup>[1,2]</sup> This location on  $\pi$  surfaces, orthogonal to the plane of the  $\pi$  system, is analogous to cation- $\pi$  interactions. The same analogy holds for dominant contributions from the quadrupole moment  $Q_{zz}$  perpendicular to the plane, negative for cation- $\pi$ , positive for anion- $\pi$  interactions, and from inward and outward in-plane dipoles from donating and withdrawing substituents, respectively.<sup>[2]</sup> Contrary to the HOMO chemistry accessible with cation- $\pi$  interactions, anion- $\pi$  interactions relate to LUMO chemistry. Like “too strong” hydrogen bonds result in proton transfer and conjugate acids and bases, “too strong” anion- $\pi$  interactions lead to charge-transfer complexes and radicals (and to nucleophilic aromatic substitutions).<sup>[1]</sup>

\* Mr. F. N. Miros, Dr. Y. Zhao,<sup>[a]</sup> Dr. G. Sargsyan,<sup>[b]</sup> Ms. M. Pupier, Dr. C. Besnard, Dr. C. Beuchat,<sup>[c]</sup> Dr. J. Mareda, Dr. N. Sakai, Prof. S. Matile  
Department of Organic Chemistry  
University of Geneva, Geneva (Switzerland)  
Fax: (+41) 22-379-3215  
E-mail: stefan.matile@unige.ch  
Homepage: www.unige.ch/sciences/chiorg/matile

[a] Present address: Institute of Polymers, ETH Zurich, Switzerland and Qingdao University of Science and Technology, China

[b] Present address: South Texas College, McAllen, Texas, USA

[c] Present address: AKYADO, Remaufens, Switzerland

Supporting information for this article is available on the WWW under <http://www.chemeurj.org/> or from the author.

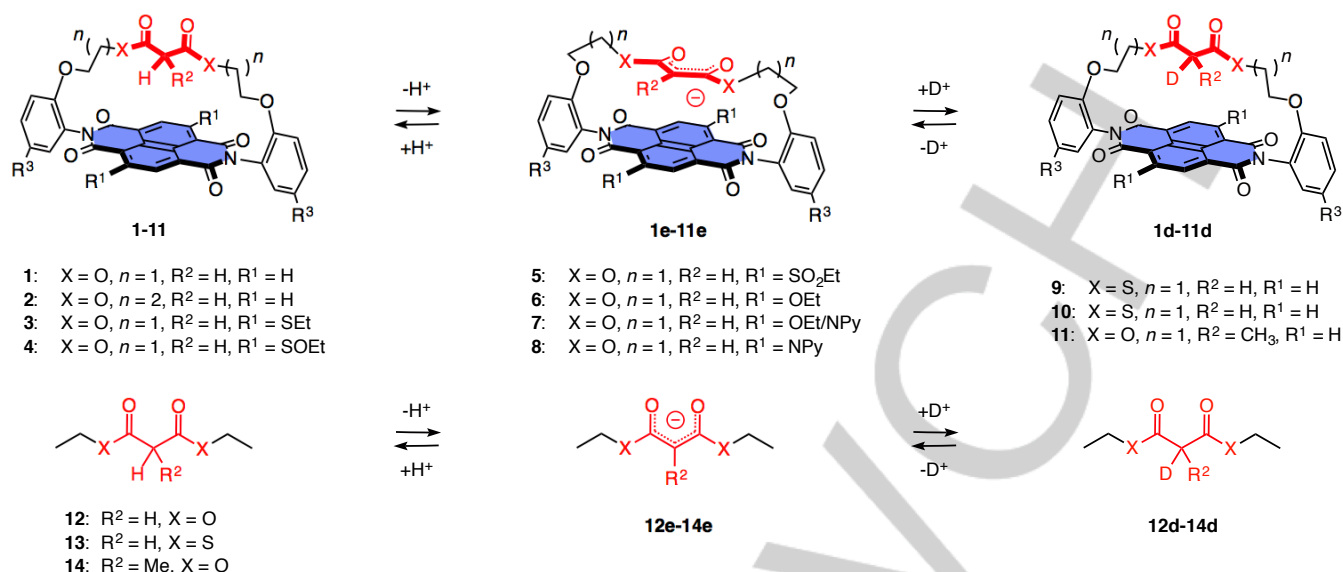


**Figure 1.** Structure of malonate-bridged NDIs **1-11**, their conjugate enolate bases **1e-11e**, deuterium exchange in CD<sub>3</sub>OD to give **1d-11d**, and controls **12-14**. R<sup>3</sup> = *tert*-butyl or *tert*-pentyl (**1**, **9**, **10**), NPy = N-pyrrolidinyl.

Experimentally, anion- $\pi$  interactions have been explored in the solid state, in solution and in the gas phase. Early focus on anion binding in solution<sup>[3]</sup> gradually shifted toward anion transport<sup>[4]</sup> and, most recently, anion- $\pi$  catalysis.<sup>[5-8]</sup> The first explicit example for anion- $\pi$  catalysis focused on the Kemp elimination, a classical model reaction with a single anionic transition state.<sup>[5]</sup> Anion- $\pi$  interactions in enolate chemistry were considered next to explore their ability to recognize the arguably most significant anionic transition states in chemistry and biology.<sup>[6]</sup> Acceleration of enolate addition to enones, nitroolefins and aldehydes on  $\pi$ -acidic surfaces has been documented, the latter continuing in an anionic cascade process with elimination and transesterification to afford coumarins.<sup>[6]</sup> In non-covalent systems, anion- $\pi$  interactions selectively catalyze disfavored enolate additions over the favored decarboxylation.<sup>[7]</sup> Asymmetric enamine catalysis on  $\pi$ -acidic surfaces has been demonstrated.<sup>[8]</sup> Moreover, contributions of anion- $\pi$  interactions to ion pairing in anion binding catalysis have been suggested recently,<sup>[13]</sup> whereas over possible contributions to enamine chemistry with MacMillan catalysts,<sup>[14]</sup> NHC chemistry with Rovis catalysts,<sup>[15]</sup> or early transamidation on perylenediimide surfaces<sup>[16]</sup> can only be speculated. Elegant computational support for remarkably rare and elusive contributions of anion- $\pi$  interactions to enzyme mechanisms has also been reported.<sup>[17]</sup>

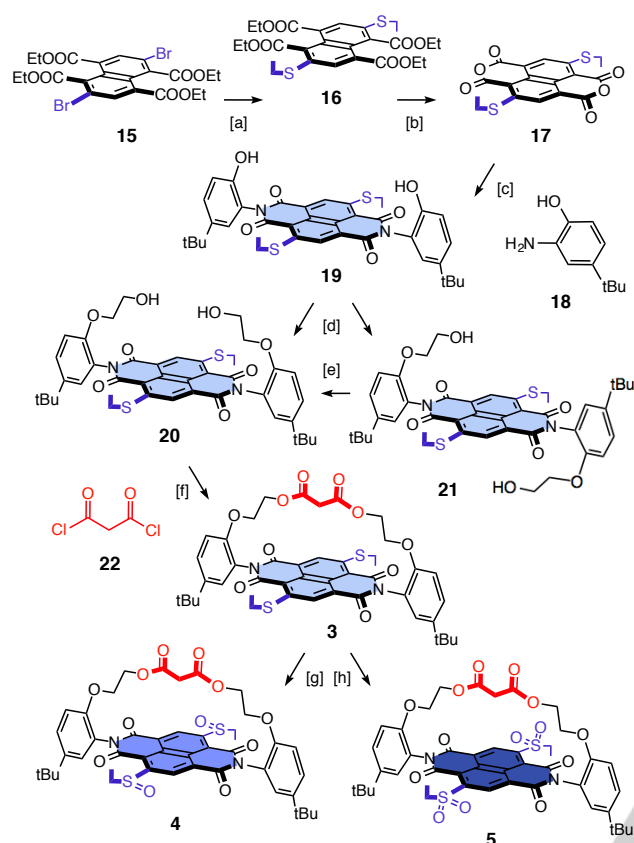
For a credible development of anion- $\pi$  catalysis, it is important to secure experimental evidence as direct as possible for the involvement and importance of anion- $\pi$  interactions in the process. This is intrinsically difficult because anion recognition occurs with reactive intermediates and transition states with delocalized negative charges. To explore anion- $\pi$  interactions in enolate chemistry with highest possible precision, we have recently proposed a synthetic strategy to position malonate dilactones covalently on the  $\pi$ -acidic surface of naphthalenediimides (NDIs).<sup>[6]</sup> Preliminary results have

confirmed that upfield shifts in the <sup>1</sup>H NMR spectra can prove the presence of the malonate on the  $\pi$  surface in dilactone **1** beyond any doubt (Figure 1). NMR titrations with base in the presence of an internal control then revealed the increase in acidity of the enol, which in turn demonstrates the stabilization of the conjugate base, that is the enolate anion, on the  $\pi$ -acidic surface. These results were important because they introduced a so far unique system to quantify enolate recognition by anion- $\pi$  interactions in solution with maximal certainty. In this report, this is done systematically. Most importantly, proton-deuterium exchange kinetics<sup>[18-20]</sup> rather than base titrations are used to determine pK<sub>a</sub> values to further minimize interference and move from conjugate bases to the stabilization of anionic transition states and reactive intermediates with anion- $\pi$  interactions.

## Results and Discussion

**Design.** The malonate-bridged NDIs **2-11** were designed based on the original system **1**, controls **12-14** were added to assure correct comparisons (Figure 1). The dependence of enolate- $\pi$  interactions on the positioning of the malonate dilactone on the  $\pi$  surface naturally had to be verified first (*n*, Figure 1). Once in place, the dependence of enolate- $\pi$  interactions and transition-state stabilization on the  $\pi$  acidity of the surface could be determined at highest possible certainty by varying R<sup>1</sup>. The dependence of enolate- $\pi$  interactions and transition-state stabilization on the nature of the enolate could be measured analogously by varying R<sup>2</sup> and X.

**Synthesis.** Malonate-bridged NDIs **2-11** were synthesized based on the procedures developed for the original system **1** on the one hand<sup>[6]</sup> and much experience with core-substituted NDIs on the other.<sup>[21-24]</sup> The preparation of NDIs **3-5** will be outlined in the following as an example (Scheme 1), details on synthesis



**Scheme 1.** Synthesis of macrodilactones **3-5**. [a] EtSH,  $K_2CO_3$ , 18-crown-6, 85 °C, 48 h, 97%. [b] 1. KOH, *i*-PrOH, 80 °C, 10 h, 70%; 2. AcOH, 85 °C, 2 h, 68%. [c] **18**, TEA, DMF, 140 °C, 10 h, 67%. [d] Bromoethanol,  $K_2CO_3$ , DMF,  $\mu$ W, 140 °C, 45 min. [e] Toluene, reflux, 1 h, 58% (d+e). [f] **22**,  $CH_2Cl_2$ , 0 °C  $\rightarrow$  rt, 5 min, 85%. [g] mCPBA (3 eq),  $CH_2Cl_2$ , 0 °C, 20 min, 62%. [h] mCPBA (10 eq),  $CH_2Cl_2$ , rt, 2 h, 88%. **3-5** and **19** are mixtures of stereoisomers unless stated otherwise ((*R,R,P*)-**4**, see below).

and characterization of all new compounds can be found in the Supplementary Information (Schemes S1-S4, Figures S10-S59).

The 2,6-dibromo naphthalene-1,4,5,8-tetraester **15** was obtained from naphthalenedianhydride following described procedures.<sup>[23,24]</sup> Nucleophilic aromatic substitution with ethanethiol gave tetraester **16** as a pure compound in excellent 97% yield. For the formation of the diimide, the anhydride **17** was reformed by ester hydrolysis under basic conditions followed by dehydration under acidic conditions. The microwave-assisted reaction of the core-substituted naphthalenedianhydride **17** with aminophenol **18** under basic conditions afforded NDI **19** in 67% yield. Williamson ether synthesis with bromoethanol gave the stable atropisomers **20** and **21**, which could be separated easily by column chromatography as reported previously for unsubstituted NDIs.<sup>[6,22]</sup> Conversion of the useless *anti* atropisomer **21** into the desired *syn* atropisomer **20** was possible by cycles of reflux in toluene and subsequent separation. The malonate-bridged NDI macrodilactone **3** was obtained by reacting the *syn* atropisomer **20** with malonyl dichloride **22**. Oxidation of the two sulfides in the core of NDI **3** with mCPBA at 0 °C gave NDI **4** with two

sulfoxides, oxidation with excess mCPBA at room temperature gave NDI **5** with two sulfones.

**Structural Studies.** Sulfides, sulfoxides and sulfones are most attractive core substituents because the  $\pi$  acidity can be varied without global structural changes (Table 1).<sup>[23]</sup> This somewhat underappreciated isostructural functional switch has been applied before not only to elaborate on anion- $\pi$  interactions<sup>[23]</sup> but also to modulate peptide secondary structures,<sup>[25]</sup> the mechanosensitivity of fluorescent probes<sup>[26]</sup> and the voltage gating of synthetic ion channels.<sup>[27]</sup> NDI **5** and NDI **4** with two sulfides and sulfones in the core exist as pairs of enantiomers, the sulfoxides in NDI **4** add two stereogenic centers at the edge of the  $\pi$  surface.<sup>[23]</sup> For NDI **4**, four peaks could be identified in chromatograms using chiral HPLC (Figure S1). For the stereoisomer eluting last at  $R_t = 13$  min, single crystals could be obtained. Structure determination by X-ray crystallography revealed the absolute configurations corresponding to (*R,R,P*)-NDI **4** (Figures 2, S2). The crystal structure of the (*R,R,P*)-dilactone **4** confirmed the position of the malonate on the  $\pi$ -acidic surface. In neutral form in the solid, the malonate carbonyls are turned away from the surface and do not show any interaction. The  $\alpha$  carbon between the malonate carbonyls was identified as tetrahedral. In neutral form in the solid, the malonate in (*R,R,P*)-NDI **4** does not exist as an enol.

The structure of macrodilactone **1** (without *tert*-pentyl solubilizers)<sup>[25]</sup> obtained from molecular modeling was nearly superimposable with crystal structure of (*R,R,P*)-NDI **4**, i.e., without strong contacts between the malonate bridge and the  $\pi$ -acidic surface (Figure 3a). This situation changed dramatically with deprotonation.

The B97D/6-311g\*\* density functional<sup>[28]</sup> within the Gaussian-09<sup>[29]</sup> package was used to model selected structures relating to malonate enolate **1e**. In the global minimum found for **1e**, the plane of the extended enolate anion was oriented parallel to the  $\pi$ -acidic surface (Figure 2, 3b). Comparable to face-to-face nitrate- $\pi$  interactions,<sup>[3,4]</sup> this parallel enolate orientation suggested that anion- $\pi$  interactions are supported by face-to-face  $\pi$ - $\pi$  interactions. In this structure, the distance from the  $\alpha$  carbon of the enolate to the aromatic plane is 0.25 Å shorter than the sum of the respective Van-der-Waals radii.

Above the face-to-face enolate **1e**, a local minimum was found at +8.94 kJ mol<sup>-1</sup> (Figure 3c). In this structure, the enolate is rotated along the long axis to promote localized interactions of the carbonyl oxyanions with the  $\pi$ -acidic surface. These oxyanion- $\pi$  interactions also occur in a minimum found at +21.30 kJ mol<sup>-1</sup> (Figure 3d). In this less favored structure, the enolate plane is nearly perpendicular with respect to the NDI plane with one carbonyl lone pair pointing into the  $\pi$  surface for maximally localized anion- $\pi$  interactions. Comparison of the full series suggested that with malonate-bridged NDIs,  $\pi$ - $\pi$ -enhanced face-to-face enolate- $\pi$  interactions with a more delocalized negative charge are preferred over edge-to-face enolate- $\pi$  interactions with the negative charge more localized on two or, at worst, one carbonyl oxygen.

**Deuterium Exchange.** Proton-deuterium exchange kinetics of 5 mM malonate-bridged NDIs **1-11** and controls **12-14** were measured by 400 or 500 MHz <sup>1</sup>H NMR spectroscopy in  $CDCl_3$  in the presence of 4% or 80%  $CD_3OD$ . Comparative studies were

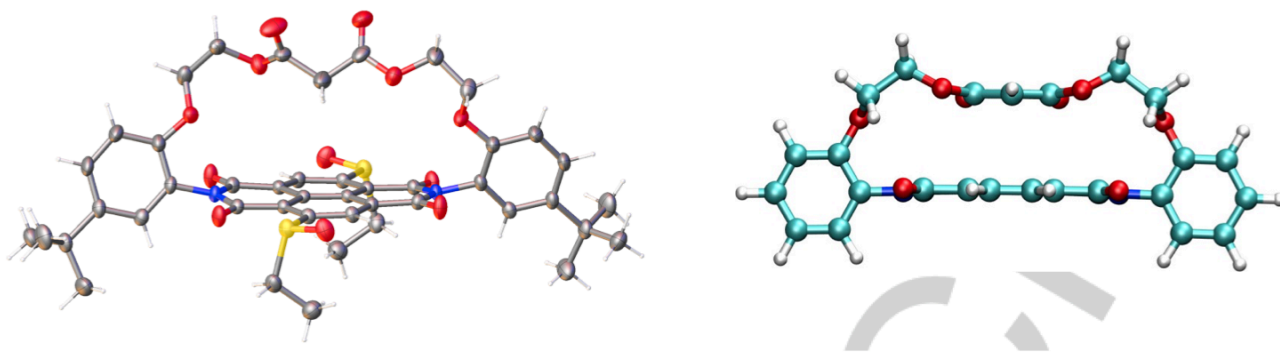


**Figure 2.** Crystal structure of malonate-bridged (*R,R,P*)-NDI **4** (left) compared to the B97D/6-311G\*\* optimized structure of enolate **1e** at the global minimum (right, without *tert*-pentyl solubilizers).

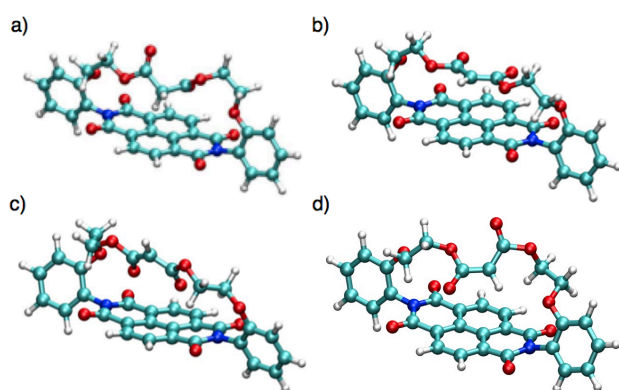


**Figure 3.** B97D/6-311G\*\* optimized structures of macrodilactone **1** (a) as well as enolate **1e** at the global minimum (b) and higher energy local minima, respectively at +8.94 kJ mol<sup>-1</sup> (c) and +21.30 kJ mol<sup>-1</sup> (d, without *tert*-pentyl solubilizers).

made with 0.01 equivalent triethylamine (TEA) to ensure that proton-deuterium exchange occurs with formation of anionic enolate intermediates **1e-14e** (Figure 1). In malonate diester control **12**, the resonance for the  $\alpha$ -CH<sub>2</sub> occurred at  $\delta = 3.88$  ppm. Exposed to the ring current above aromatic surfaces,<sup>[30]</sup> the  $\alpha$ -CH<sub>2</sub> peak shifted upfield by up to  $\Delta\delta = -1.75$  ppm (Table 1, entry 6). Consistent with reports in the literature,<sup>[18-20]</sup> the  $\alpha$ -CHD resonance appeared just upfield of the  $\alpha$ -CH<sub>2</sub> peak ( $\Delta\delta \sim -0.02$  ppm, Figure 4). As observed previously with other substrates,<sup>[18,19]</sup> the H-D coupling pattern was usually not resolved (Figures 4, S3-S6).<sup>[31]</sup> These  $\alpha$ -CHD peaks increased at the beginning of H-D exchange but disappeared with continuing exchange to the NMR-silent  $\alpha$ -CD<sub>2</sub> product (Figures 4, S3-S6).

Deuterium exchange kinetics were determined from the decrease of the  $\alpha$ -CH<sub>2</sub> signals relative to a non-exchanging signal and the appearance and disappearance of the  $\alpha$ -CHD signals with time (Figures 4, 5a, S3-S7). Changes of reaction rates on  $\pi$  surfaces in macrodilactones were obtained by comparing absolute rate constants with those of acyclic controls **12-14** (Table 1). Rate changes  $k_{\text{rel}}$  were converted into changes

in activation energy  $\Delta\Delta G_{\text{TS}}$ . These changes could originate from the stabilization or destabilization of anionic transition states (TS) on  $\pi$ -acidic or  $\pi$ -basic surfaces. Contributions from ground-state (de)stabilization to changes in activation energies cannot be excluded either without data from Michaelis-Menten kinetics.<sup>[5]</sup>

The stabilization of enolate intermediates **1e-11e** themselves, *i.e.*  $\Delta\Delta G_{\text{RI}}$ , was approximated from the acidity of the malonate macrodilactones **1-11**. Richard analysis was used to extract  $pK_{\text{a}}$ 's from deuterium exchange kinetics.<sup>[18]</sup> This method has been validated previously for a broad variety of enolates.<sup>[18-20]</sup> In brief, rate constants obtained for controls were plotted against their known  $pK_{\text{a}}$  (Figures S8, S9). The rate constants identified for the new, malonate dilactones **1-11** on NDI surfaces were then added to the respective Richard correlation plot to extract an estimate of their  $pK_{\text{a}}$  (Table 1).

**Methods Validation.** Deuterium exchange kinetics were explored first with the known malonate dilactone **1** (Table 1, entries 6 and 7). In this original macrocycle, the malonate is positioned on the  $\pi$  surface of a native NDI without additional substituents in the core. Compared to acyclic diethylmalonate **12**, H-D exchange in dilactone **1** on a native NDI surface was 16.2 times faster in the presence of 1 M CD<sub>3</sub>OD (4%) in CDCl<sub>3</sub> (Figure 5a, O vs X; Table 1, entry 6). With 20 M (or 80%) CD<sub>3</sub>OD in CDCl<sub>3</sub>, the relative rate enhancement on  $\pi$ -acidic surfaces in **1** naturally decreased slightly to  $k_{\text{rel}} = 8.6$  (Table 1, entry 7).

Malonate **12** and methylmalonate **14** were used as controls with known  $pK_{\text{a}}$  to develop one Richard correlation plot for fast H-D exchange with 20 M CD<sub>3</sub>OD (80%) and another one for slow H-D exchange with 1 M CD<sub>3</sub>OD (4%) in CDCl<sub>3</sub> (Figures S8, S9). Their application to the rate enhancements  $k_{\text{rel}}$  measured for dilactone **1** at different concentrations of CD<sub>3</sub>OD gave reasonably similar  $pK_{\text{a}} = 14.3$  and  $pK_{\text{a}} = 14.6$  (Table 1, entries 6 and 7). Small changes in enolate stabilization in response to changes in solvent polarity were expected. The  $pK_{\text{a}} = 14.6$  obtained from H-D exchange in CDCl<sub>3</sub> with only 4% CD<sub>3</sub>OD was nearly identical with the  $pK_{\text{a}} = 14.5$  obtained previously with base titrations in CDCl<sub>3</sub> (Table 1, entry 6).<sup>[6]</sup>

These consistent results with known controls validated H-D exchange in general and Richard correlation plots<sup>[18]</sup> in particular

**Table 1.** Deuterium exchange data for malonate dilactones on  $\pi$ -acidic surfaces.<sup>[a]</sup>

entry	Cpd <sup>[b]</sup>	<i>n</i>	X	R <sup>2</sup>	R <sup>1</sup>	<i>E</i> <sub>LUMO</sub> (eV) <sup>[c]</sup>	$\Delta\delta$ (ppm) <sup>[d]</sup>	<i>k</i> <sub>rel</sub> <sup>[e,f]</sup>	$\Delta\Delta G_{TS}$ (kJ mol <sup>-1</sup> ) <sup>[g]</sup>	<i>pK</i> <sub>a</sub> <sup>[h,i]</sup>	$\Delta pK_a$ <sup>[j]</sup>	$\Delta\Delta G_{RI}$ (kJ mol <sup>-1</sup> ) <sup>[k]</sup>
1	<b>5</b>	1	O	H	SO <sub>2</sub> Et	-4.63	-2.34	1971 <sup>[e]</sup>	-18.8	10.9 <sup>[h]</sup>	-5.5	-13.6
2 <sup>[l]</sup>	( $\delta_3$ )- <b>4</b>	1	O	H	SOEt	-4.42	-1.88	1752 <sup>[e]</sup>	-18.5	11.0 <sup>[h]</sup>	-5.4	-13.3
3 <sup>[l]</sup>	( $\delta_1$ )- <b>4</b>	1	O	H	SOEt	-4.42	-1.53	1683 <sup>[e]</sup>	-18.4	11.1 <sup>[h]</sup>	-5.3	-13.2
4 <sup>[l]</sup>	( $\delta_4$ )- <b>4</b>	1	O	H	SOEt	-4.42	-2.13	731 <sup>[e]</sup>	-16.3	11.7 <sup>[h]</sup>	-4.7	-11.7
5 <sup>[l]</sup>	( $\delta_2$ )- <b>4</b>	1	O	H	SOEt	-4.42	-1.57	195 <sup>[e]</sup>	-13.1	12.0 <sup>[h]</sup>	-4.4	-10.8
6	<b>1</b>	1	O	H	H	-4.13	-1.75	16.2 <sup>[e]</sup>	-6.9	14.6 <sup>[h]</sup>	-1.8	-4.5
7	<b>1</b>	1	O	H	H	-4.13	-1.75	8.60 <sup>[f]</sup>	-5.3	14.3 <sup>[i]</sup>	-2.1	-5.2
8	<b>6</b>	1	O	H	OEt	-3.99	-2.23	1.30 <sup>[f]</sup>	-0.7	15.5 <sup>[i]</sup>	-0.9	-2.2
9	<b>7</b>	1	O	H	NPy, OEt	-3.83	-2.08	0.49 <sup>[f]</sup>	+1.8	16.6 <sup>[i]</sup>	+0.2	+0.5
10	<b>3</b>	1	O	H	SEt	-4.02	-2.22	0.27 <sup>[f]</sup>	+3.2	16.7 <sup>[i]</sup>	+0.3	+0.7
11	<b>8</b>	1	O	H	NPy	-3.71	-2.15	0.015 <sup>[f]</sup>	+10.4	17.6 <sup>[i]</sup>	+1.2	+3.0
12	<b>2</b>	2	O	H	H	-4.13	-0.81	0.06 <sup>e</sup>	+7.0	18.4 <sup>[i]</sup>	+2.0	+5.0
13	<b>9</b>	1	S	H	H	-4.13	-1.00	5.36 <sup>e</sup>	-4.2	10.9 <sup>[h]</sup>	-1.3	-3.2
14	<b>10</b>	1	O	CH <sub>3</sub>	H	-4.13	-2.15	0.076 <sup>f</sup>	+6.4	18.7 <sup>[h]</sup>	+0.7	+1.7
15	<b>11</b>	1	O	CH <sub>3</sub>	SO <sub>2</sub> Et	-4.63	-1.47	63.2 <sup>f</sup>	-10.3	16.8 <sup>[i]</sup>	-1.2	-3.0

[a] Measured by 400 or 500 MHz <sup>1</sup>H NMR spectroscopy in CDCl<sub>3</sub> with 5 mM substrate, 50  $\mu$ M TEA and 4% (1 M)<sup>[e,h]</sup> or 80% (20 M) CD<sub>3</sub>OD<sup>[f,i]</sup> at room temperature. [b] For structures, see Figure 1. [c] LUMO energy levels of NDIs in eV relative to -5.1 eV for Fc<sup>+/0</sup>/Fc, extrapolated from literature values and control measurements.<sup>[23,24]</sup> [d] Shift of the  $\alpha$ -CH<sub>2</sub> compared to **12** (3.88 ppm, for **1-8**), **13** (3.78 ppm, for **9**) and **14** (3.41 ppm, for **10-11**). [e] Relative rate constants with 4% (1 M) CD<sub>3</sub>OD<sup>[a]</sup> compared to **12-14**. [f] Relative rate constants with 80% (20 M) CD<sub>3</sub>OD<sup>[a]</sup> compared to **12-14**. [g] Transition-state (de)stabilization (or ground-state (de)stabilization), from  $\Delta\Delta G_{TS} = -RT \ln(k_{rel})$ . [h] Acidity of the malonate esters, approximated<sup>[15]</sup> from  $pK_a = c \log(k/p)$ , *p* = number of protons, *c* from fit with known *pK<sub>a</sub>* and *k* measured for **1**, **12** and **14** with 4% (1 M) CD<sub>3</sub>OD.<sup>[a]</sup> [i] Same, approximated from *pK<sub>a</sub>* and *k* measured for **12** and **14** with 80% (20 M) CD<sub>3</sub>OD.<sup>[a]</sup> [j] Change in apparent acidity compared to **12** (16.4; for **1-8**), **13** (12.2, for **9**) and **14** (18.0, for **10-11**). [k] (De)stabilization of the reactive enolate intermediate (RI) on  $\pi$  surfaces, from  $\Delta\Delta G_{RI} = RT(\Delta pK_a)$ . [l] Diastereomers, labeled with increasing upfield shift, ( $\delta_1$ )-**4** contains (*R,R,P*)-**4** (see Figure 6, all chiral compounds are measured as mixtures of stereoisomers).

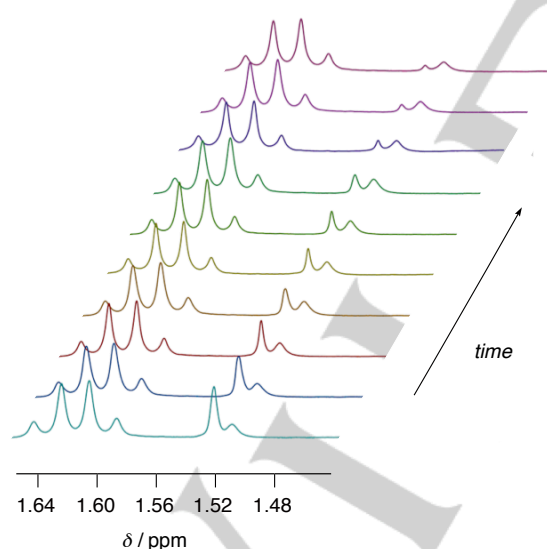


**Figure 4.** Evolution with time of the <sup>1</sup>H NMR spectrum of **1** in CDCl<sub>3</sub> with 4% CD<sub>3</sub>OD (50  $\mu$ M TEA, room temperature, 1.62 ppm = *tert*-pentyl CH<sub>2</sub>, 1.52 ppm =  $\alpha$ -CH<sub>2</sub>, 1.51 ppm =  $\alpha$ -CHD).

as the least interfering method to probe anion- $\pi$  interactions in covalent systems with meaningful accuracy. Moreover, they provided corroborative support for the stabilization of enolate intermediates on  $\pi$ -acidic surfaces and added experimental

evidence for transition-state stabilization by anion- $\pi$  interactions. These results are particularly valuable because the reaction takes place with  $\alpha$ -CH<sub>2</sub> carbons whose protons appear at  $\delta = 1.52$  ppm rather than at  $\delta = 3.88$  ppm (Figure 4). This upfield shift of  $\Delta\delta = -1.75$  ppm is observed throughout the entire exchange process (Figure 4) and thus provides experimental evidence as direct as possible that the acceleration of the reaction of interest occurs indeed on the  $\pi$ -acidic aromatic surface.

**Positioning.** Compared to the original malonate dilactone **1**, the expanded macrocycle **2** contains two more methylenes in the malonate bridge (*n* = 2, Figure 1). The resonance for the  $\alpha$ -CH<sub>2</sub> in the <sup>1</sup>H NMR spectrum of the ring-expanded macrodilactone **2** was  $\Delta\delta = -0.81$  ppm compared to the acyclic diester **12** (Table 1, entry 12). The upfield shift for the original macrodilactone **1** was  $\Delta\delta = -1.75$  ppm (Table 1, entry 6). This reduced exposure to the aromatic ring current<sup>[30]</sup> indicated that in the ring-expanded macrodilactone **2**, the  $\alpha$ -CH<sub>2</sub> is not in very close proximity of the  $\pi$  surface.

Contrary to the acceleration on the  $\pi$ -acidic surface in the matched macrodilactone **1** (*k*<sub>rel</sub> = 16.2), H-D exchange in the expanded macrocycle **2** slowed down significantly (Table 1, entry 12). Deceleration far beyond anion- $\pi$  free control **12** (*k*<sub>rel</sub> = 0.06) suggested that in mismatched macrodilactone **2**, both transition state ( $\Delta\Delta G_{TS} = +7.0$  kJ mol<sup>-1</sup>) and reactive enolate intermediate ( $\Delta\Delta G_{RI} = +5.0$  kJ mol<sup>-1</sup>) are destabilized rather than stabilized. This result confirmed that the mismatched bridge in macrocycle **2** is too long to exist in relaxed extended conformation. This strained, tight folding not only prevents the enolate to approach the  $\pi$  surface for stabilizing anion- $\pi$  interactions but also hinders the spatially demanding planarization from the *sp*<sup>3</sup> hybridized

acid to the  $sp^2$  hybridized conjugate enolate base (Figures 1 and 2). The clear difference found between the operational macrolactone **1** and the dysfunctional homolog **2** supported that the design of the former is appropriate to explore enolate chemistry on  $\pi$ -acidic surfaces. Molecular models confirmed that bridges shorter than in dilactone **1** would result in highly strained macrocycles ( $n < 1$ , Figure 1).

**$\pi$  Acidity.** After validation of the design of macrocycles **1** to position malonates on  $\pi$  surfaces, a series of six dilactones **3-8** with different substituents in the NDI core was prepared (Table 1). As a measure of  $\pi$  acidity, quadrupole moments  $Q_{zz}$  were not appropriate because the reduced symmetry with sulfoxide and sulfone substituents hinders calculations.<sup>[23]</sup> The energy levels of the LUMO of the NDIs, experimentally accessible by cyclic voltammetry measurements, were used as reasonable approximation instead.<sup>[23,24]</sup> The  $\pi$ -acidity gradient built to probe the acceleration of H-D exchange in malonates with anion- $\pi$  interactions covers 920 meV in seven steps in total. The most  $\pi$ -acidic surface was prepared with strongly withdrawing sulfones in NDI core in dilactone **5** ( $E_{LUMO} = -4.63$  eV), the least  $\pi$ -acidic one with strongly donating amines in NDI core in macrocycle **8** ( $E_{LUMO} = -3.71$  eV, Table 1). The intermediate steps in the seven-component  $\pi$ -acidity gradient were covered with withdrawing sulfoxides in **4** ( $E_{LUMO} = -4.42$  eV), hydrogens in **1** ( $E_{LUMO} = -4.13$  eV) and donating sulfides in **3** ( $E_{LUMO} = -4.02$  eV), ethers in **6** ( $E_{LUMO} = -3.99$  eV), ethers/amines in **7** ( $E_{LUMO} = -3.83$  eV, Table 1, entries 1-11).

In the  $^1\text{H}$  NMR spectrum of macrolactone **1**, the upfield shift  $\Delta\delta = -1.75$  ppm of the resonance of the  $\alpha$ - $\text{CH}_2$  provided direct experimental evidence that the malonate is correctly positioned on the  $\pi$ -acidic NDI surface (Table 1, entry 6). With core substituents, this upfield shift generally increased. The strongest upfield shift  $\Delta\delta = -2.34$  ppm was found for the most  $\pi$ -acidic macrocycle **5** (Table 1, entry 1). However, differences were overall small and a clear correlation of upfield shifts and  $\pi$  acidity could not be identified.

The velocity of H-D exchange increased with increasing  $\pi$  acidity of the NDI. On the most  $\pi$ -acidic surface in dilactone **5**, the stabilization of the transition state reached  $\Delta\Delta G_{TS} = -18.1$  kJ mol $^{-1}$  (Table 1, entry 1, Figure 5a, ● vs X). The Brønsted acidity of the malonate increased by  $\Delta pK_a = -5.5$  to a  $pK_a = 10.9$ . From the increase in Brønsted acidity, a  $\Delta\Delta G_{RI} = -13.6$  kJ mol $^{-1}$  was calculated for enolate stabilization by intramolecular anion- $\pi$  interactions with the most  $\pi$ -acidic surface in dilactone **5** (Table 1, entry 1). A  $pK_a = 10.9$  of the malonate at maximal  $\pi$  acidity in macrocycle **5** is in the range of the Brønsted acidity of phenols or alkylammonium cations. For comparison, a  $\Delta pK_a = -5.5$  corresponds to the deprotonation of an arginine residue ( $pK_a = 12.5$ ) in neutral water.<sup>[12]</sup> Contrary to the deprotonation of lysine residues ( $pK_a = 10.5$ ,  $\Delta pK_a = -3.5$ ), the deprotonation of arginine residues is considered as “impossible” in biology, and the permanent nature of the positive charge is thought to account for much of what is generally referred to as “arginine magic”.<sup>[12]</sup>

In the full seven-component gradient established with macrocycles **1/3-8**, the increase of the Brønsted acidity of the malonate with increasing  $\pi$  acidity of the NDI surface was linear with two most intriguing exceptions (Figure 5b). The first clear deviation from linearity concerned NDI **3** with sulfide substituents in the core (Figure 5b, filled circle, Table 1, entry 10). H-D Exchange was clearly slower than expected from the LUMO level.

This apparent underperformance of NDI **3** was intriguing because the donating power of sulfides changes with the electron density in the aromatic system. With electron-rich aromatics, sulfides are ineffective or even very weak acceptors, as reflected in their Hammett  $\sigma_p = +0.03$ .<sup>[32]</sup> With increasing  $\pi$  acidity, sulfides become increasingly strong donor.<sup>[33]</sup> The found deviation from linearity suggested that, intriguingly, this increasing donor strength of sulfides with increasing  $\pi$  acidity might affect anion- $\pi$  interactions more than redox potentials. The second deviation from linearity concerned sulfoxides **4**. Unavoidable because H-D exchange is stereoselective (see below), it turned out that the least active stereoisomer ( $\delta_2$ )-**4** obeys linear dependence (Table 1, entry 5), whereas the additional chirality at the edge of the  $\pi$ -surface accelerated H-D exchange with all other stereoisomers beyond expectations (Figure 5, dashed circle, Table 1, entries 2-4).

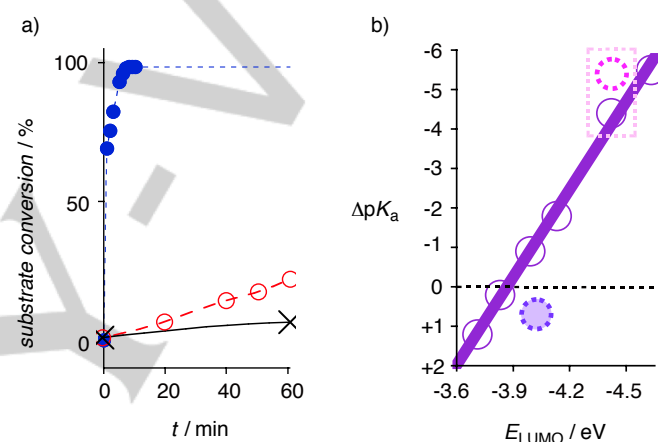


**Figure 5.** (a) Representative  $^1\text{H}$  NMR kinetics for deuterium exchange in the fastest macrocycle **5** (●), the original **1** (○), and control **12** (X) in the presence of 4%  $\text{CD}_3\text{OD}$  in  $\text{CDCl}_3$  (0.01 equivalent TEA, room temperature, Table 1). (b) Dependence of the  $\Delta pK_a$  of malonates **1/3-8** (vs control **12**, dashed line) on the LUMO energy of the NDIs in the macrolactones. Linear curve fit is added with the only intention to guide the eye, and deviations from linearity are indicated for **3** (filled dashed circle) and the most active diastereomer of **4** (empty dashed circle).

The linear dependence of malonate  $pK_a$  on  $\pi$  acidity should not be overinterpreted considering that the values at low  $\pi$  acidity had to be measured at higher solvent polarity (i.e.,  $\text{CDCl}_3$  with 80% rather than 4%  $\text{CD}_3\text{OD}$  to accelerate H-D exchange, see above, Table 1). Nevertheless, nearly identical  $pK_a$ 's measured for **1** under the two different conditions (4% vs 80%  $\text{CD}_3\text{OD}$  in  $\text{CDCl}_3$ ) suggested that the observed trends are meaningful (Table 1, entries 6 and 7). Macrocycle **6** with  $E_{LUMO} = -3.99$  eV was the least  $\pi$ -acidic system that accelerated H-D exchange (Table 1, entry 8). Macrocycle **7** with  $E_{LUMO} = -3.83$  eV was the most  $\pi$ -acidic system to decelerate H-D exchange (Table 1, entry 9; except for the outlier **3**, see above). This inversion from activation to inhibition was interesting because all NDIs present in the seven-component gradient have positive quadrupole moments. Even the strongly decelerating macrocycle **8** with  $E_{LUMO} = -3.71$  eV remains slightly  $\pi$ -acidic ( $Q_{zz} = +2.3$  B $^{[24]}$ ). The inversion from enolate stabilization to enolate destabilization occurred below the  $Q_{zz} = +8.0$  B $^{[24]}$  of dilactone **6**. This  $\pi$  acidity of NDIs with two alkoxy groups in the core is still respectable, in

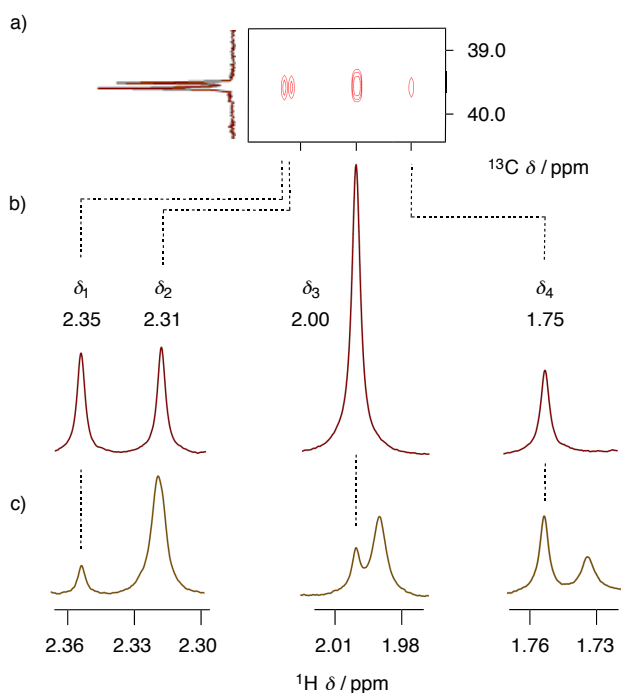


**Figure 6.** (a) Part of  $^{13}\text{C}$ ,  $^1\text{H}$  HSQC NMR spectra of **4** with correlation of  $\alpha\text{-CH}_2$  signals for all stereoisomers. Below are parts of  $^1\text{H}$  NMR spectrum of **4** in  $\text{CDCl}_3$  (b) at the time of and (c) 2 minutes after the addition of 4%  $\text{CD}_3\text{OD}$  (50  $\mu\text{M}$  TEA, room temperature).

the range of the classical  $\pi$  acid hexafluorobenzene ( $Q_{zz} = +9.5$  B).<sup>[24]</sup> The strong dependence in the seven-component  $\pi$ -acidic gradient with inversion of activity below  $Q_{zz} = +8$  B thus provided quantitative experimental support for the notion that *strongly  $\pi$ -acidic surfaces with  $Q_{zz} > +10$  B are essential to observe significant activities with anion- $\pi$  interactions in solution.*

**Stereoselectivity.** Macrodilactones **4** contain highly  $\pi$ -acidic NDIs with chiral sulfoxides in the core (Table 1, entries 2-5, Figure 2). According to  $^{13}\text{C}$ ,  $^1\text{H}$  HSQC NMR spectra, the  $\alpha\text{-CH}_2$  gave two peaks at 39.6 ppm in the  $^{13}\text{C}$  NMR spectra, whereas the  $^1\text{H}$  NMR spectra of the mixture of stereoisomers showed four separate  $\alpha\text{-CH}_2$  peaks between 2.35 and 1.75 ppm (Figures 6a, S26-S28). The four diastereomers corresponding to the four signals were labeled with increasing upfield shift from  $(\delta_1)\text{-4}$  with  $\delta = 2.35$  ppm to  $(\delta_4)\text{-4}$  with  $\delta = 1.75$  ppm (Figure 6b). Each diastereomer contains one pair of enantiomers, the  $\alpha\text{-CH}_2$  peak of  $(R,R,P)\text{-4}$  was at 1.75 ppm, i.e., part of  $(\delta_4)\text{-4}$ . Consistent with the strong  $\pi$  acidity of the NDI surface with two sulfoxides in the core, deuterium exchange rates were fast for all diastereomers of **4** (Table 1, entries 2-5). For diastereomers  $(\delta_3)\text{-4}$  and  $(\delta_4)\text{-4}$ , the  $\alpha\text{-CHD}$  resonance could be observed upfield of the  $\alpha\text{-CH}_2$  peak (Figure 6c). Possibly overlapping with the  $\alpha\text{-CH}_2$  signal, the  $\alpha\text{-CHD}$  peak of diastereomers  $(\delta_1)\text{-4}$  and  $(\delta_2)\text{-4}$  was not detectable (Figure 6c). The representative  $^1\text{H}$  NMR spectrum taken two minutes after  $\text{CD}_3\text{OD}$  addition (4% in  $\text{CDCl}_3$ ) showed that the deuterium exchange kinetics of the four diastereomers differ significantly. Diastereomers  $(\delta_1)\text{-4}$  and  $(\delta_3)\text{-4}$  exchanged fast, whereas  $(\delta_4)\text{-4}$  and particularly  $(\delta_2)\text{-4}$  were much slower. These differences demonstrated that deuterium exchange, i.e., enolate- $\pi$  interactions on chiral  $\pi$  acidic surfaces, is stereoselective. The

best chiral sulfoxides  $(\delta_3)\text{-4}$  were with  $\text{p}K_a = 11.0$  almost as good as the more  $\pi$ -acidic sulfones in macrodilactone **5** (Table 1, entries 1 vs 2). The worst sulfoxides  $(\delta_2)\text{-4}$  were with  $\text{p}K_a = 12.0$  one order of magnitude weaker (Table 1, entries 2 vs 5).

**Thiomalonates.** Reduced resonance between carbonyl and sulfur increases the acidity of the  $\alpha$ -protons of thioesters compared to oxoesters.<sup>[7,34]</sup> The reactivity of their enolates increases correspondingly.<sup>[7,34]</sup> In macrocycle **9**, the malonate oxolactones of the original macrocycle **1** are replaced by thiolactones (Table 1, entry 13). In the  $^1\text{H}$  NMR spectrum of thioester control **13**, the resonance for the  $\alpha\text{-CH}_2$  occurred at  $\delta = 3.78$  ppm, that is  $\Delta\delta = -0.10$  ppm upfield of less acidic oxoester control **12**. On the  $\pi$ -acidic surface in the thiolactone **9**, the  $\alpha\text{-CH}_2$  of the malonate was upfield shifted by  $\Delta\delta = -1.00$  ppm compared to thioester control **13** (Table 1, entry 13). This upfield shift was small compared to the  $\Delta\delta = -1.75$  ppm found for malonates on the same  $\pi$ -acidic surface in the homologous dioxolactone **1** (Table 1, entry 6). The origin of this difference is unclear but probably related to differences in intrinsic Brønsted acidity rather than to ring expansion with the longer C-S bonds ( $\sim 1.2$  Å in total).

Deuterium exchange with thioester control **13** was faster than with oxoester **12**. Richard correlation plots afforded a  $\text{p}K_a = 12.2$  for malonate dithioester **13** in  $\text{CDCl}_3$  with 4%  $\text{CD}_3\text{OD}$ . Compared to this fast exchanging thiomalonate **13**, deuterium exchange on  $\pi$ -acidic surfaces in thiolactone **9** was still 5.36 times faster (Table 1, entry 13). This rate enhancement calculated to an increase in Brønsted acidity by  $\Delta\text{p}K_a = -1.3$  to a  $\text{p}K_a = 10.9$ , that is a stabilization of the enolate intermediate on the  $\pi$ -acidic surface by  $\Delta\Delta G_{\text{RI}} = -3.2$  kJ mol $^{-1}$  (Table 1, entry 13). With  $\text{p}K_a = 10.9$ , the Brønsted acidity of malonate dithiolactones on  $\pi$  surfaces of intermediate  $\pi$  acidity in **9** was as strong as that of malonate dioxolactones on surfaces of maximal  $\pi$  acidity in **5** (Table 1, entries 1 and 13). At identical  $\pi$  acidity, enolate stabilization by  $\Delta\Delta G_{\text{RI}} = -3.2$  kJ mol $^{-1}$  for malonate dithiolactones in **9** was quite comparable to the  $\Delta\Delta G_{\text{RI}} = -4.7$  kJ mol $^{-1}$  for malonate dioxolactones in **1** (Table 1, entries 6 and 13). Intrinsically better enolate stabilization by resonance in dithiomalonates compared to dioxomalonates could account for the slightly weaker contributions of anion- $\pi$  interactions to the former.

**Methylmalonates.** The positioning of methylmalonates on  $\pi$ -acidic surfaces in macrodilactone **10** caused the  $\alpha\text{-CH}$  resonance to shift upfield by  $\Delta\delta = -2.15$  ppm (Table 1, entry 14). This compared to homolog **1** clearly stronger upfield shift suggested that the bulky methyl group forces the small  $\alpha\text{-CH}$  into close contact with the repulsive  $\pi$ -acidic surface. With  $k_{\text{rel}} = 0.076$ , deuterium exchange with methylmalonates in dilactone **10** was much slower than with methylmalonate diester control **14** (Table 1, entry 14). Analog to the sterically hindered intercalation and face-to-face  $\pi$ -stacking with toluene compared to benzene, the methyl group in  $\alpha$ -position should hinder the formation of the most favored co-planar enolate- $\pi$  interaction in **1/3-8** (Figures 2, 3b).

To accelerate H-D exchange also with the disfavored methylmalonates, they were placed on  $\pi$  surfaces of maximal  $\pi$  acidity in dilactone **11**. With increasing  $\pi$  acidity, the strong upfield shift  $\Delta\delta = -2.15$  ppm of the  $\alpha\text{-CH}$  in **10** decreased to a subaverage  $\Delta\delta = -1.47$  ppm in **11** (Table 1, entries 14 and 15). H-D exchange on the most  $\pi$ -acidic surface in **11** indeed accelerated despite the presence of the methyl group in  $\alpha$  position (Table 1, entry 15). However, enolate stabilization on

most  $\pi$ -acidic surfaces with methyl malonate remained with  $\Delta\Delta G_{\text{RI}} = -3.0 \text{ kJ mol}^{-1}$  clearly inferior compared to the  $\Delta\Delta G_{\text{RI}} = -13.6 \text{ kJ mol}^{-1}$  obtained with the methyl-free homolog **5** (Table 1, entries 1 and 15).

## Conclusions

The objective of this study was to explore possible contributions of anion- $\pi$  interactions to catalysis with highest possible certainty. The challenge is to secure experimental evidence as direct as possible for or against the stabilization of anionic transition states and reactive intermediates on  $\pi$ -acidic aromatic surfaces. To tackle this challenge, macrodilactone architectures are introduced to place malonates covalently on the  $\pi$ -acidic surface of NDIs. Their presence on the  $\pi$  surface is directly detectable by upfield shifts in the  $^1\text{H}$  NMR spectra, also in action, *i.e.*, during deuterium exchange. Deuterium exchange is implemented as least interfering process to probe enolate intermediates as well as transition states on  $\pi$ -acidic surfaces. The results provide extensive corroborative support that enolates and their respective transition states are stabilized on  $\pi$ -acidic surfaces.

The most important specific lessons learned are the following. Firstly, the reported results in support of existence and significance of anion- $\pi$  catalysis are unique with regard to the level of precision and confidence that is accessible with the introduced covalent approach. Secondly, the  $\Delta pK_{\text{a}} = -5.5$  determined for maximized enolate- $\pi$  interactions under these conditions is significant. Thirdly, the introduced  $\pi$ -acidity gradient composed of seven components covering almost 1 eV exceeds previously explored gradients by far. This seven-component gradient was essential to find the inversion of activity below  $Q_{\text{zz}} = +8 \text{ B}$  and thus secure quantitative experimental evidence that strong  $\pi$  acids with  $Q_{\text{zz}} > +10 \text{ B}$  are required to create function with anion- $\pi$  interactions. It is important to realize that this cut-off is around classical  $\pi$  acids such as hexafluorobenzene ( $Q_{\text{zz}} = +9.5 \text{ B}$ ).<sup>[24]</sup> With weaker  $\pi$  acids with  $Q_{\text{zz}} < +10 \text{ B}$ , contributions are weak, and similarly weak repulsive components begin to dominate. This result will be important for future developments.<sup>[7,8]</sup> Last but not least, the found stereoselectivity of deuterium exchange in malonates on chiral  $\pi$  surfaces is most intriguing, also with regard to future perspectives with asymmetric anion- $\pi$  catalysis.<sup>[8]</sup> The result is particularly valuable because the selectivity originates directly from chirality within the  $\pi$ -acidic surface.

## Acknowledgements

We thank the NMR and the Sciences Mass Spectrometry (SMS) platforms for services, and the University of Geneva, the European Research Council (ERC Advanced Investigator), the National Centre of Competence in Research (NCCR) Molecular Systems Engineering, the NCCR Chemical Biology and the Swiss NSF for financial support.

**Keywords:** Anion- $\pi$  interactions • enolates • deuterium exchange • macrocycles • stereoselectivity • acidity •

[1] In this study, the term anion- $\pi$  interaction refers to the site of the interaction (*i.e.*, on the aromatic  $\pi$  surface) without any implications on the nature of the interaction.<sup>[2-8]</sup>

[2] a) D. Quinonero, C. Garau, C. Rotger, A. Frontera, P. Ballester, A. Costa, P. M. Deya, *Angew. Chem. Int. Ed.* **2002**, *41*, 3389-3392; b) M.

- Mascal, A. Armstrong, M. D. Bartberger, *J. Am. Chem. Soc.* **2002**, *124*, 6274-6276; c) I. Alkorta, I. Rozas, J. Elguero, *J. Am. Chem. Soc.* **2002**, *124*, 8593-8598; d) A. Frontera, P. Gamez, M. Mascal, T. J. Mooibroek, J. Reedijk, *Angew. Chem. Int. Ed.* **2011**, *50*, 9564-9583; e) H. T. Chifotides, K. R. Dunbar, *Acc. Chem. Res.* **2013**, *46*, 894-906; f) P. Gamez, T. J. Mooibroek, S. J. Teat, J. Reedijk, *Acc. Chem. Res.* **2007**, *40*, 435-444; g) L. M. Salonen, M. Ellermann, F. Diederich, *Angew. Chem. Int. Ed.* **2011**, *50*, 4808-4842; h) H.-J. Schneider, *Acc. Chem. Res.* **2013**, *46*, 1010-1019; i) S. E. Wheeler, J. W. G. Bloom, *J. Phys. Chem. A* **2014**, *118*, 6133-6147; k) B. P. Hay, R. Custelcean, *Cryst. Growth. Des.* **2009**, *9*, 2539-2545; l) P. Gamez, T. J. Mooibroek, S. J. Teat, J. Reedijk, *Acc. Chem. Res.* **2007**, *40*, 435-444; m) M. Giese, M. Albrecht, K. Rissanen, *Chem. Rev.* **2015**, *115*, 8867-8895.
- [3] a) L. Adriaenssens, G. Gil-Ramirez, A. Frontera, D. Quinonero, E. C. Escudero-Adan, P. Ballester, *J. Am. Chem. Soc.* **2014**, *136*, 3208-3218; b) D.-X. Wang, M.-X. Wang, *J. Am. Chem. Soc.* **2013**, *135*, 892-897; c) M. Giese, M. Albrecht, G. Ivanova, A. Valkonen, K. Rissanen, *Supramol. Chem.* **2012**, *24*, 48-55; d) M. Barceló-Oliver, A. Bauzá, B. A. Baquero, A. García-Raso, A. Terrón, E. Molins, A. Frontera, *Tetrahedron Lett.* **2013**, *54*, 5355-5360; e) M. M. Watt, L. N. Zakharov, M. M. Haley, D. W. Johnson, *Angew. Chem. Int. Ed.* **2013**, *52*, 10275-10280; f) Q. He, Y. Han, Y. Wang, Z.-T. Huang, D.-X. Wang, *Chem. Eur. J.* **2014**, *20*, 7486-7491; g) A. Bretschneider, D. M. Andrada, S. Dechert, S. Meyer, R. A. Mata, F. Meyer, *Chem. Eur. J.* **2013**, *19*, 16988-17000; h) S. T. Schneebeli, M. Frascioni, Z. Liu, Y. Wu, D. M. Gardner, N. L. Strutt, C. Cheng, R. Carmielli, M. R. Wasielewski, J. F. Stoddart, *Angew. Chem. Int. Ed.* **2013**, *52*, 13100-13104; i) P. Arranz-Mascros, C. Bazzicalupi, A. Bianchi, C. Giorgi, M.-L. Godino-Salido, M.-D. Gutierrez-Valero, R. Lopez-Garzo, M. Savastano, *J. Am. Chem. Soc.* **2013**, *135*, 102-105; j) M. G. Chudzinski, C. A. McClary, M. S. Taylor, *J. Am. Chem. Soc.* **2011**, *133*, 10559-10567; k) D.-X. Wang, Q. Y. Zheng, Q. Q. Wang, M.-X. Wang, *Angew. Chem. Int. Ed.* **2008**, *47*, 7485-7488. l) P. S. Lakshminarayanan, I. Ravikumar, E. Suresh, P. Ghosh, *Inorg. Chem.* **2007**, *46*, 4769-4771; m) H. Maeda, T. Morimoto, A. Osuka, H. Furuta, *Chem. Asian J.* **2006**, *1*, 832-844; n) Y. S. Rosokha, S. V. Lindeman, S. V. Rosokha, J. K. Kochi, *Angew. Chem. Int. Ed.* **2004**, *43*, 4650-4652; o) N. Busschaert, M. Wenzel, M. E. Light, P. Iglesias-Hernandez, R. Perez-Tomas, P. A. Gale, *J. Am. Chem. Soc.* **2011**, *133*, 14136-14148.
- [4] a) V. Gorteau, G. Bollot, J. Mareda, A. Perez-Velasco, S. Matile, *J. Am. Chem. Soc.* **2006**, *128*, 14788-14789; b) A. Vargas Jentzsch, A. Hennig, J. Mareda, S. Matile, *Acc. Chem. Res.* **2013**, *46*, 2791-2800; c) L. Adriaenssens, C. Estarellas, A. Vargas Jentzsch, M. Martinez Belmonte, S. Matile, P. Ballester, *J. Am. Chem. Soc.* **2013**, *135*, 8324-8330; d) A. Vargas Jentzsch, S. Matile, *J. Am. Chem. Soc.* **2013**, *135*, 5302-5303; e) Q. He, Y. F. Ao, Z. T. Huang, D.-X. Wang, *Angew. Chem. Int. Ed.* **2015**, *54*, 11785-11790.
- [5] a) Y. Zhao, Y. Domoto, E. Orentas, C. Beuchat, D. Emery, J. Mareda, N. Sakai, S. Matile, *Angew. Chem. Int. Ed.* **2013**, *52*, 9940-9943; b) Y. Zhao, C. Beuchat, J. Mareda, Y. Domoto, J. Gajewy, A. Wilson, N. Sakai, S. Matile, *J. Am. Chem. Soc.* **2014**, *136*, 2101-2111; c) T. Lu, S. E. Wheeler, *Org. Lett.* **2014**, *16*, 3268-3271.
- [6] Y. Zhao, N. Sakai, S. Matile, *Nat. Commun.* **2014**, *5*, 3911.
- [7] Y. Zhao, S. Benz, N. Sakai, S. Matile, *Chem. Sci.* **2015**. DOI 10.1039/C5SC02563J.
- [8] Y. Zhao, Y. Cotellet, A.-J. Avestro, N. Sakai, S. Matile, *J. Am. Chem. Soc.* **2015**, *137*, 11582-11585.
- [9] a) D. A. Dougherty, *Acc. Chem. Res.* **2013**, *46*, 885-893; b) A. S. Mahadevi, G. N. Sastry, *Chem. Rev.* **2013**, *113*, 2100-2138.
- [10] a) K. U. Wendt, G. E. Schulz, E. J. Corey, D. R. Liu, *Angew. Chem. Int. Ed.* **2000**, *39*, 2812-2833; b) S. Yamada, J. S. Fossey, *Org. Biomol. Chem.* **2011**, *9*, 7275-7281; c) D. A. Stauffer, R. E. Barrans Jr., D. A. Dougherty, *Angew. Chem. Int. Ed.* **1990**, *29*, 915-918; d) P. Lakshminarasimhan, R. B. Sunoj, J. Chandrasekhar, V. Ramamurthy, *J. Am. Chem. Soc.* **2000**, *122*, 4815-4816; e) I. Neda, P. Sakhaii, A. Wassmann, U. Niemeyer, E. Günther, J. Engel, *Synthesis* **1999**, 1625-1632; f) L. Yao, J. Aubé, *J. Am. Chem. Soc.* **2007**, *129*, 2766-2767; g) R. R. Knowles, S. Lin, E. N. Jacobsen, *J. Am. Chem. Soc.* **2010**, *132*, 5030-5032; h) Q. Zhang, K. Tiefenbacher, *Nat. Chem.* **2015**, *7*, 197-202.

- [11] a) K. Fujisawa, C. Beuchat, M. Humbert-Droz, A. Wilson, T. A. Wesolowski, J. Mareda, N. Sakai, S. Matile, *Angew. Chem. Int. Ed.* **2014**, *53*, 11266-11269; b) K. Fujisawa, M. Humbert-Droz, R. Letrun, E. Vauthey, T. A. Wesolowski, N. Sakai, S. Matile, *J. Am. Chem. Soc.* **2015**, *137*, 11047-11056; c) M. Mitra, P. Manna, S. K. Seth, A. Das, J. Meredith, M. Helliwell, A. Bauzá, S. R. Choudhury, A. Frontera, S. Mukhopadhyay, *Cryst. Eng. Comm.* **2013**, *15*, 686-696.
- [12] G. Gasparini, E.-K. Bang, J. Montenegro, S. Matile, *Chem. Commun.* **2015**, *51*, 10389-10402.
- [13] A. Berkessel, S. Das, D. Pekel, J.-M. Neudörfl, *Angew. Chem. Int. Ed.* **2014**, *53*, 11660-11664.
- [14] a) M. C. Holland, J. B. Metternich, C. Mück-Lichtenfeld, R. Gilmour, *Chem. Commun.* **2015**, *50*, 13906-13909; b) I. K. Mangion, A. B. Northrup, D. W. C. MacMillan, *Angew. Chem. Int. Ed.* **2004**, *43*, 6722-6724.
- [15] U. V. Harit, P. Wheeler, T. Rovis, *Adv. Synth. Catal.* **2012**, *354*, 1617-1639.
- [16] C. M. Rojas, J. Rebek Jr., *J. Am. Chem. Soc.* **1998**, *120*, 5120-5121.
- [17] a) C. Estarellas, A. Frontera, D. Quiñero, P. M. Deya, *Angew. Chem., Int. Ed.* **2011**, *50*, 415-418; b) A. Bauza, D. Quinonero, P. M. Deya, A. Frontera, *Chem. Eur. J.* **2014**, *20*, 6985-6990.
- [18] A. Rios, T. L. Amyes, J. P. Richard, *J. Am. Chem. Soc.* **2002**, *124*, 8251-8259.
- [19] A. Rios, T. L. Amyes, J. P. Richard, *J. Am. Chem. Soc.* **2000**, *122*, 9373-9385.
- [20] a) P.-J. Um, D. G. Drueckhammer, *J. Am. Chem. Soc.* **1998**, *120*, 5605-5610; b) T. L. Amyes, J. P. Richard, *J. Am. Chem. Soc.* **1992**, *114*, 10297-10302; c) T. L. Amyes, J. P. Richard, *J. Am. Chem. Soc.* **1996**, *118*, 3129-3141; d) D. Wilson, N. R. Branda, *Angew. Chem. Int. Ed.* **2012**, *51*, 5431-5434; e) D. A. Alonso, S. Kitagaki, N. Utsumi, C. F. Barbas III, *Angew. Chem. Int. Ed.* **2008**, *47*, 4588-4591; f) S. M. Cope, D. Taylor, R. W. Nagorski, *J. Org. Chem.* **2011**, *76*, 380-390.
- [21] a) S. V. Bhosale, C. H. Jani, S. J. Langford, *Chem. Soc. Rev.* **2008**, *37*, 331-342; b) F. Würthner, M. Stolte, *Chem. Commun.* **2011**, *47*, 5109-5115; c) E. L. Suraru, F. Würthner, *Angew. Chem. Int. Ed.* **2014**, *53*, 7428-7448; d) N. Sakai, P. Charbonnaz, S. Ward, S. Matile, *J. Am. Chem. Soc.* **2014**, *136*, 5575-5578; e) M. B. Avinash, P. K. Samanta, K. V. Sandeepa, S. K. Pati, T. Govindaraju, *Eur. J. Org. Chem.* **2013**, 5838-5847; f) F. Doria, I. Manet, V. Grande, S. Monti, M. Freccero, *J. Org. Chem.* **2013**, *78*, 8065-8073; g) Y. Fukutomi, M. Nakano, J.-Y. Hu, I. Osaka, K. Takimiya, *J. Am. Chem. Soc.* **2013**, *135*, 11445-11448; h) F. Zhang, Y. Hu, T. Schuettfort, C.-A. Di, X. Gao, C. R. McNeill, L. Thomsen, S. C. B. Mannsfeld, W. Yuan, H. Sirringhaus, D. Zhu, *J. Am. Chem. Soc.* **2013**, *135*, 2338-2349; i) G. Sforzini, E. Orentas, A. Bolag, N. Sakai, S. Matile, *J. Am. Chem. Soc.* **2013**, *135*, 12082-12090; j) J. Chang, Q. Ye, K.-W. Huang, J. Zhang, Z.-K. Chen, J. Wu, C. Chi, *Org. Lett.* **2012**, *14*, 2964-2967; k) N. Ponnuswamy, G. D. Pantos, M. M. J. Smulders, J. M. K. Sanders, *J. Am. Chem. Soc.* **2012**, *134*, 566-573; l) M. R. Molla, S. Ghosh, *Chem. Eur. J.* **2012**, *18*, 9860-9869; m) S. Tu, S. H. Kim, J. Joseph, D. A. Modarelli, J. L. Parquette, *J. Am. Chem. Soc.* **2011**, *133*, 19125-19130; n) X. Zhan, A. Facchetti, S. Barlow, T. J. Marks, M. A. Ratner, M. R. Wasielewski, S. R. Marder, *Adv. Mater.* **2011**, *23*, 268-284; o) M. Lista, J. Areephong, N. Sakai, S. Matile, *J. Am. Chem. Soc.* **2011**, *133*, 15228-15231; p) N. Sakai, S. Matile, *J. Am. Chem. Soc.* **2011**, *133*, 18542-18545; q) S. Guha, S. Saha, *J. Am. Chem. Soc.* **2010**, *132*, 17674-17677; r) S. Hagihara, H. Tanaka, S. Matile, *J. Am. Chem. Soc.* **2008**, *130*, 5656-5657; s) P. Talukdar, G. Bollot, J. Mareda, N. Sakai, S. Matile, *Chem. Eur. J.* **2005**, *11*, 6525-6532; t) B. Abraham, S. McMasters, M. A. Mullan, L. A. Kelly, *J. Am. Chem. Soc.* **2004**, *126*, 4293-4300; u) F. Würthner, S. Ahmed, C. Thalacker, T. Debaerdemaeker, *Chem. Eur. J.* **2002**, *8*, 4742-4750; v) G. J. Gabriel, B. L. Iverson, *J. Am. Chem. Soc.* **2002**, *124*, 15174-15175.
- [22] a) Y. S. Chong, B. E. Dial, W. G. Burns, K. D. Shimizu, *Chem. Commun.* **2012**, *48*, 1296-1298; b) K. D. Shimizu, T. M. Dewey, J. Rebek Jr., *J. Am. Chem. Soc.* **1994**, *116*, 5145-5149.
- [23] a) J. Misek, A. Vargas Jentzsch, S. Sakurai, D. Emery, J. Mareda, S. Matile, *Angew. Chem. Int. Ed.* **2010**, *49*, 7680-7683; b) N.-T. Lin, A. Vargas Jentzsch, L. Guénée, J.-M. Neudörfl, S. Aziz, A. Berkessel, E. Orentas, N. Sakai, S. Matile, *Chem. Sci.* **2012**, *3*, 1121-1127; c) Y. Zhao, G. Huang, C. Besnard, J. Mareda, N. Sakai, S. Matile, *Chem. Eur. J.* **2015**, *21*, 6202-6207.
- [24] a) R. S. K. Kishore, O. Kel, N. Banerji, D. Emery, G. Bollot, J. Mareda, A. Gomez-Casado, P. Jonkheijm, J. Huskens, P. Maroni, M. Borkovec, E. Vauthey, N. Sakai, S. Matile, *J. Am. Chem. Soc.* **2009**, *131*, 11106-11116; b) N. Sakai, J. Mareda, E. Vauthey, S. Matile, *Chem. Commun.* **2010**, *46*, 4225-4237.
- [25] a) J. R. Kramer, T. J. Deming, *J. Am. Chem. Soc.* **2014**, *136*, 5547-5550; b) X. Miao, W. Cao, W. Zheng, J. Wang, X. Zhang, J. Gao, C. Yang, D. Kong, H. Xu, L. Wang, Z. Yang, *Angew. Chem. Int. Ed.* **2013**, *52*, 7781-7785; c) E. L. Dane, S. B. King, T. M. Swager, *J. Am. Chem. Soc.* **2010**, *132*, 7758-7768; d) C. Wolschner, A. Giese, H. A. Kretzschmar, R. Huber, L. Moroder, N. Budisa, *Proc. Natl. Acad. Sci. USA.* **2009**, *106*, 7756-7761; e) N. Sakai, S. Matile, *J. Am. Chem. Soc.* **2002**, *124*, 1184-1185; f) N. Sakai, S. Matile, *Chem. Eur. J.* **2000**, *6*, 1731-1737; g) G. P. Dado, S. H. Gellman, *J. Am. Chem. Soc.* **1993**, *115*, 12609-12610.
- [26] a) M. Dal Molin, Q. Verolet, A. Colom, R. Letrun, E. Derivery, M. Gonzalez-Gaitan, E. Vauthey, A. Roux, N. Sakai, S. Matile, *J. Am. Chem. Soc.* **2015**, *137*, 568-571; b) M. Dal Molin, Q. Verolet, S. Soleimanpour, S. Matile, *Chem. Eur. J.* **2015**, *21*, 6012-6021.
- [27] a) N. Sakai, D. Gerard, S. Matile, *J. Am. Chem. Soc.* **2001**, *123*, 2517-2524; b) N. Sakai, D. Houdebert, S. Matile, *Chem. Eur. J.* **2003**, *9*, 223-232.
- [28] S. J. Grimme, *Comput. Chem.* **2006**, *27*, 1787-1799.
- [29] M. J. Frisch, *et al*, *Gaussian 09, Revision C.01*, Gaussian Inc., Wallingford CT, **2013**.
- [30] O. Zerbe, S. Jurt, *Applied NMR Spectroscopy for Chemists and Life Scientists*, Wiley-VCH, Weinheim, **2013**. p 36.
- [31] Ref [30], p 335-349.
- [32] a) L. P. Hammett, *J. Am. Chem. Soc.* **1937**, *59*, 96-103; b) C. Hansch, A. Leo, R. W. Taft, *Chem. Rev.* **1991**, *91*, 420-427.
- [33] F. Bernardi, A. Mangini, N. D. Epitotis, J. R. Larson, S. Shaik, *J. Am. Chem. Soc.* **1977**, *99*, 7465-7470.
- [34] a) S. P. Bew, R. G. Stephenson, J. Rouden, L. A. Martinez-Lozano, H. Seylani, *Org. Lett.* **2013**, *15*, 3805-3807; b) W. Yang, D. G. Drueckhammer, *J. Am. Chem. Soc.* **2001**, *123*, 11004-11009.

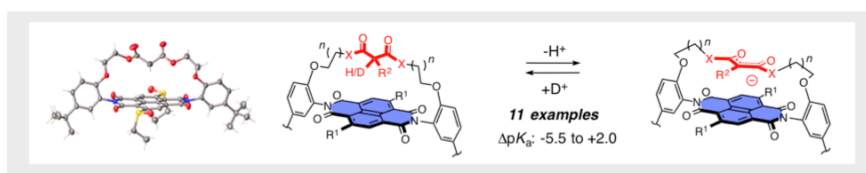
Received: ((will be filled in by the editorial staff))

Revised: ((will be filled in by the editorial staff))

Published online: ((will be filled in by the editorial staff))

Entry for the Table of Contents

FULL PAPER



**Beyond uncertainty:** Tied up onto chiral  $\pi$  surfaces in solution, stereoselective proton-deuterium exchange is directly followed by  $^1\text{H}$  NMR spectroscopy to see malonate acidity increase along a seven-component  $\pi$ -acidity gradient up to 5.5 orders of magnitude - commonly considered as impossible in biology -, to quantify the stabilization of anionic reactive intermediates and transition states on  $\pi$ -acidic surfaces, and to secure direct experimental evidence for the long suspected: that really strong  $\pi$  acids are needed to catch anion- $\pi$  interactions at work.

### Supramolecular Chemistry

François N. Miros, Yingjie Zhao, Gevorg Sargsyan, Marion Pupier, Céline Besnard, César Beuchat, Jiri Mareda, Naomi Sakai and Stefan Matile\*



**Enolate Stabilization by Anion- $\pi$  Interactions: Deuterium Exchange in Malonate Dilactones on  $\pi$ -Acidic Surfaces**